Opposing functions of β-arrestin 1 and 2 in Parkinson's disease via microglia inflammation and Nprl3

Yinquan Fang
Nanjing Medical University
Qingling Jiang
Nanjing Medical University
Shanshan Li
Nanjing University of Chinese Medicine
Hong Zhu
Nanjing Medical University
Xiao Ding
Nanjing University of Chinese Medicine
Rong Xu
Nanjing Midical University
Miaomiao Chen
Nanjing Midical University
Nanshan Song
Nanjing Medical University
Mengmeng Song
Nanjing University of Chinese Medicine
Jianhua Ding
Nanjing Medical University
Ming Lu
Nanjing Medical University
Guangyu Wu
Augusta University
Gang Hu (ghu@njucm.edu.cn)
Nanjing Medical University

Research article

Keywords: Parkinson's disease, β-arrestins, microglia activation, neuroinflammation, Nprl3

Posted Date: May 7th, 2020

DOI: https://doi.org/10.21203/rs.3.rs-24932/v1

Version of Record: A version of this preprint was published at Cell Death & Differentiation on March 8th, 2021. See the published version at https://doi.org/10.1038/s41418-020-00704-9.

Abstract

Background

Although β-arrestins (ARRBs) regulate diverse physiological and pathophysiological processes, their function and regulation in Parkinson's disease (PD) remain poorly defined.

Methods

We measured expression of ARRB1 and ARRB2 in liposaccharide (LPS)-induced and 1-methyl-4-phenyl-1, 2, 3, 6-tetrahydropyridine (MPTP)-induced PD mice. ARRB1-deficient and ARRB2-deficient mouse were used to assess the impact of ARRBs on dopaminergic (DA) neuron loss and microglia activation in PD mouse models. After primary mouse DA neurons were exposed to the conditioned medium from ARRB1 knockdown or ARRB2 knockout microglia stimulated by LPS plus interferon γ (IFN-γ), the degeneration of DA neurons was quantified. Gain- and loss-of-function studies were used to study the effects of ARRBs on microglia activation *in vitro*. To further understand the mechanism, we measured the activation of classical inflammatory pathways and used RNA sequencing to identify the novel downstream effector of ARRBs.

Result

In this study, we demonstrate that expression of ARRB1 and ARRB2, particularly in microglia, is reciprocally regulated in PD mouse models. ARRB1 ablation ameliorates, whereas ARRB2 knockout aggravates, the pathological features of PD, including DA neuron loss, neuroinflammation and microglia activation *in vivo*, as well as microglia-mediated neuron damage and inflammation *in vitro*. In parallel, ARRB1 and ARRB2 produce adverse effects on the activation of inflammatory signal transducers and activators of transcription 1 (STAT1) and nuclear factor-κB (NF-κB) pathways in microglia. We also show that two ARRBs competitively interact with activated p65 in the NF-κB pathway and that nitrogen permease regulator-like 3 (Nprl3), a functionally poorly characterized protein, is a novel effector acting downstream of both ARRBs.

Conclusion

Collectively, these data demonstrate that two closely related ARRBs have completely opposite functions in microglia-mediated inflammatory responses, via Nprl3, and differentially affect the pathogenesis of PD, and suggest a potential therapeutic strategy.

Background

Parkinson's disease (PD) is the second most common neurodegenerative disorder after Alzheimer's disease (AD), and affects approximately 2–3% of the world's population over the age of 65 [1, 2]. Although the etiology and pathogenic mechanism of PD are not fully understood, a variety of genetic factors and environmental exposures have been identified to contribute to the pathological progression of PD, and the possible mechanisms include the changes in dopamine metabolism, mitochondrial dysfunction, endoplasmic reticulum stress, impaired autophagy and deregulated immunity [3]. Chronic neuroinflammation in the substantia nigra pars compacta (SNc), the progressive loss of dopaminergic (DA) neurons in SNc, and the presence of Lewy bodies in different nuclei of the nervous system are the neuropathological hallmarks of PD [4].

Microglia are the main immune cells of the brain and their activation-mediated inflammatory processes in PD have been investigated extensively [5, 6]. It is now increasingly apparent that sustained microglia activation is a major contributor to neuroinflammation and responsible for exacerbated neurodegeneration in PD [7, 8]. One of the characteristics of activated microglia is the enhanced production of pro-inflammatory cytokines, such as tumor necrosis factor α (TNFα), interleukin (IL) 1β, IL-6 and interferon-γ (IFN-γ), which are toxic to DA neurons [9–12]. Activated microglia, as well as concentration of pro-inflammatory factors, are increased in the SNc of PD patients [13–15]. Therefore, identification of the regulators involved in microglia activation may create new avenues for drug design in the treatment of PD.

β-Arrestins (ARRBs) are originally identified to mediate the desensitization and intracellular trafficking of G protein-coupled receptors (GPCRs) [16–21]. There are two ARRB isoforms, ARRB1 and ARRB2; they share 78% amino acid identity. It is now widely appreciated that both ARRBs may serve as important signal transducers and scaffolds to control multiple intracellular signaling cascades in a GPCR-dependent or independent fashion [22–25], with the inflammatory nuclear factor-κB (NF-κB) pathway being a well-studied example in which ARRBs may directly interact with pathway components [26–28].

There is considerable evidence supporting the diverse roles of ARRBs in the pathogenesis of central nervous system diseases, such as ischemia, AD and multiple sclerosis [29–33]. Several recent studies have also implied a role for ARRB2 in PD. For example, ARRB2 in microglia mediates the functions of dynorphin/κ-opioid receptors in controlling endotoxin-elicited pro-inflammatory responses and protecting tyrosine hydroxylase (TH) positive neurons from inflammation-induced toxicity [34]. ARRB2 is involved in the development of L-DOPA-induced dyskinesia [35]. Studies from our laboratory have shown that ARRB2 negatively regulates the assembly and activation of NOD-like receptor protein-3 (NLRP3) via direct interaction in astrocytes, which contributes to the anti-neuroinflammatory effect of dopamine D2 receptors in PD [36]. However, noting is known about the functions of ARRB1 in the pathological progression of PD.

The purposes of this study are to investigate the possible functions of both ARRB1 and ARRB2 in the pathogenesis of PD and to elucidate the underlying mechanisms. We demonstrate that by virtue of their abilities to differentially regulate nitrogen permease regulator-like 3 (Nprl3) and the NF-κB and signal

transducers and activators of transcription 1 (STAT1) pathways in microglia, ARRB1 and ARRB2 opposingly affect DA neuron degeneration and microglia inflammation both *in vitro* and *in vivo*. These data not only reveal novel functions and regulatory mechanisms of ARRBs in PD but also suggest a potential therapeutic approach for the disease.

Methods

Antibodies and reagents.

Antibodies against ARRB1 (cat# 12697), ARRB2 (3857), iNOS (13120), p-p65 (3033), p65 (8242), p-IKKβ (2697), IKKβ (8943), p-STAT1 (7649), STAT1 (14995), and Bax (2772) were purchased from Cell Signaling Technologies (CST); CD206 (AF2534) antibodies and all ELISA kits from R&D Systems; Bcl-2 (40639) antibodies from Signalway Antibody; TH (T1299) and β-actin (A1978) antibodies, LPS, MPTP, poly-L-lysine (PLL), bovine serum albumin (BSA), Triton X-100 and Hoechst 33324 from Sigma; ARRB1 (53780) and ARRB2 (514791) antibodies from Santa Cruz; Nprl3 (NBP1-88447) antibodies from Novus Biologicals; Iba-1 (019-19741) antibodies from Wako, Japan; CD16 (553142) antibodies from BD Biosciences; NeuN (ab177487) and GFAP (ab7260) antibodies from Abcam; Alexa-conjugated secondary antibodies, LipofectamineTM RNAi MAX, Lipofectamine 3000, TRIzol reagent and DAPI from Invitrogen; trypsin, EDTA, DMEM/F-12 medium, fetal bovine serum (FBS), DMEM medium, streptomycin, penicillin, sodium pyruvate, neurobasal medium, B27, and glutamine from Gibco; granulocyte-macrophage colony stimulating factor (GM-CSF) and IFN-γ from PeproTech; protease inhibitor cocktail and FastStart Universal SYBR Green Master from Roche; TaKaRa Master Mix from TaKaRa, Japan; DAB staining system from Boster, China; cell counting kit-8 (CCK-8) from Dojindo, China; protein-A/G beads from Thermo Scientific; the GFP-tagged ARRB1 and Nprl3 plasmids from GeneChem Co.; all siRNAs from GenePharma, China.

Animals and PD models.

Arrb1 $^{-/-}$ mice were purchased from the Jackson Laboratory (Las Vegas, NV) and *Arrb2*$^{-/-}$ mice kindly provided by Dr. Gang Pei (Tongji University, Shanghai, China). C57BL/6J WT mice were from the Animal Core Faculty of Nanjing Medical University. All mice were allowed access to food and water ad libitum and maintained at 22 to 24 °C with a 12 h light/dark cycle.

The LPS- and MPTP-induced PD models were developed as described previously [36, 37]. Briefly, mice (male, 3–4 months old, $n = 11$ for each genotype) were microinjected bilaterally with LPS (0.5 μg in 1 μl of saline, Sigma) at the SNc (AP: -3.0 mm; ML: ± 1.3 mm; DV: -4.2 mm) at a rate of 0.2 μl/min in a stereotaxic apparatus or administered with MPTP (20 mg/kg, i.p., Sigma) 4 times at 2-h intervals. After 7 days, the mice were sacrificed, and the brain tissues extracted and processed for immunoblotting, PT-PCR and immunohistochemistry.

Isolation and treatment of primary cells.

Primary microglia were isolated from the brain tissues of neonatal mice (within 3 days after birth) by treatment with 0.25% trypsin/EDTA as described [38]. The cells were plated into PLL-coated T75 flasks and cultured in DMEM/F-12 medium containing 1% penicillin/streptomycin and 10% FBS. The medium was changed every 3 days. After 10–14 days, the cells were split onto plates, incubated in serum-free base medium for 1 h, and treated with LPS (100 ng/ml) plus IFN-γ (20 ng/ml) at 37 °C for 24 h. The CM was collected and centrifuged at 12,000 g for 10 min at 4 °C and the supernatant was used to treat DA neurons.

BMDMs were isolated from the femur and tibia cavities of mice (male, 3 months old) and cultured in DMEM supplemented with 10% FBS, 1% streptomycin/penicillin, 1 mM sodium pyruvate and 10 ng/ml GM-CSF as described [39]. The medium was changed every 3 days and the cells were used for further experiments after 7 days.

DA neurons were prepared from ventral mesencephalon of fetuses (E15-16) by treatment with 0.125% trypsin/EDTA as described previously [40]. The neurons were cultured in neurobasal medium supplemented with 2% B27 and 0.5 mM glutamine for 6 days and treated with microglial CM (microglia CM:neurobasal = 1:2) for 24 h.

Cell transfection.

In knockdown experiments, primary cells were transfected with individual siRNAs targeting ARRB1, ARRB2 or Nprl3 (Additional file 1, Table. S1) using LipofectamineTM RNAi MAX. In overexpression experiments, the cells were transfected with GFP-tagged ARRB1, ARRB2 or Nprl3 in the pcDNA3.1 vector using Lipofectamine 3000.

Western blotting.

Tissues or cells were lysed in RIPA buffer containing protease inhibitor cocktail. The lysates were centrifuged at 16,000 g for 15 min at 4 °C, and the supernatants were used for immunoblotting on 8–12% gels using antibodies against ARRB1 (1:800 dilution), ARRB2 (1:1000), iNOS (1:1000), CD206 (1:1000), p-p65 (1:1000), p65 (1:1000), p-IKKβ (1:1000), IKKβ (1:1000), p-STAT1 (1:1000), STAT1 (1:1000), Bcl-2 (1:500), Bax (1:1000), TH (1:2000), ARRB1 (1:500), ARRB2 (1:500), Nprl3 (1:1000) or β-actin (1:5000). The blots were analyzed using ImageQuant™ LAS 4000 imaging (GE Healthcare, USA) and Bio-Rad Gel Doc XR documentation systems.

ELISA.

The concentrations of cytokines, including TNF-α, IL-1β and IL-6, in the supernatants of BMDMs were measured using ELISA kits, according to the manufacturer's instructions.

Quantitative RT-PCR.

Total RNA extracted from mouse tissues or cells with TRIzol reagent was reverse transcribed with the TaKaRa Master Mix. The cDNAs obtained were mixed with FastStart Universal SYBR Green Master and gene-specific primers (Additional file 2, Table. S2) for RT-PCR in a StepOnePlus instrument (Applied Biosystems, USA). GAPDH served as an internal control.

Immunohistochemistry.

Frozen 30-μm-thick midbrain sections or primary DA neurons were deparaffinized by treatment with 3% H_2O_2 for 30 min, blocked by 5% BSA plus 0.3% Triton X-100 for 60 min, and then incubated with anti-TH (1:1000) or anti-Iba-1(1:1000) antibodies at 4 °C overnight as described [37]. After washing, the slides were incubated with secondary antibodies (1:1000) for 60 min. After staining with the DAB system and imaging in a stereomicroscope (Olympus, Japan), the axon lengths were measured and the positive cells in the SNc were stereologically counted by Microbrightfield Stereo-Investigator software (Microbrightfield, USA)

Immunofluorescence.

Immunofluorescence staining was carried out as described previously [41]. Frozen 20-μm-thick brain sections and BMDMs were fixed with 4% PFA for 30 min, blocked with 5% BSA and then incubated with antibodies against CD16 (1:200), ARRB1 (1:50), ARRB2 (1:50), Iba-1 (1:1000), NeuN (1:800) or GFAP (1:800) at 4 °C overnight, followed by incubation with Alexa 594- or Alexa 555-conjugated secondary antibodies (1:500) for 1 h. The slides were stained with Gold antifade reagent with DAPI, and visualized under fluorescence microscopes (Nikon TE2000-S, Melville, NY or Zeiss LSM700, Oberkochen, Germany).

Hoechst staining.

Neurons were fixed with 4% PFA (Paraformaldehyde) for 30 min and stained with Hoechst 33324 for 10 min (1:1000). Apoptotic neurons were quantified by imaging in a fluorescence microscope (Olympus BX 60).

Cell viability.

The cell viability of primary neurons was measured using CCK-8, according to the manufacturer's instructions.

Co-IP.

BMDMs were lysed in RIPA buffer containing protease inhibitors as described [39]. The cell extracts were pre-cleared with protein-A/G beads and then immunoprecipitated with 2 μg of antibodies against ARRB1 or ARRB2 at 4 °C overnight followed by incubation with protein A/G beads at 4 °C for 2.5 h. After washing for 3 times with RIPA buffer, the bound proteins were eluted and detected by immunoblotting.

RNA-seq.

Total RNA was extracted from primary microglia with TRIzol reagent. RNA-seq libraries were prepared and sequenced on an Illumina HiSeq 4000 system by Novogene. Differential expression analyses were performed by DESeq.

Statistical analysis.

Statistical tests were carried out using GraphPad Prism 7.0 software. Unpaired Student's t test was used for comparison between two groups. One-way analysis of variance (ANOVA) or two-way repeated-measures ANOVA were used to assess differences among multiple groups. Data are presented as the means ± s.e. Differences were considered statistically significant at $P < 0.05$.

Results

Differential expression of ARRBs in PD mouse models.

As an initial approach to define the functions of ARRBs in PD, we measured their expression in the midbrain of LPS- and MPTP-induced PD mouse models [42]. ARRB1 and its mRNA were increased by approximately 150%, whereas ARRB2 and its mRNA were decreased by more than 50%, in LPS-induced PD model (Fig. 1a-c). Such opposite regulation of ARRB1 and ARRB2 expression was also observed in MPTP-induced PD model (Fig. 1a-c). More interestingly, immunostaining showed that both ARRBs were highly expressed in Iba-1$^+$ microglia (Fig. 1d), but barely in GFAP$^+$ astrocytes (Additional file 3: Figure S1a) and NeuN$^+$ neurons (Additional file 3: Figure S1b) in the SNc of LPS- and MPTP-induced PD mice. Consistent with their expression in PD models *in vivo*, ARRB1 expression was markedly augmented, whereas ARRB2 expression was attenuated in primary cultures of microglia after LPS plus IFN-γ stimulation (Fig. 1e-f). These data suggest that the expression of ARRB1 and ARRB2, particularly in microglia, is differentially regulated in both inflammation- and toxin-induced mouse models of PD.

Effects of ARRB knockout on DA neuron loss, microglia activation and neuroinflammation in PD models in vivo.

We then used *Arrb1*$^{-/-}$ and *Arrb2*$^{-/-}$ knockout mice to generate PD mouse models by LPS or MPTP challenge and studied DA neuron loss and microglia activation in the SNc. Ablation of ARRB1 or ARRB2 was confirmed by immunoblotting and one isoform knockout did not affect the expression of the other isoform (Additional file 3: Figure S2). As expected, LPS challenge caused remarkable DA neuron death and microglia activation as measured by staining with antibodies against TH and Iba-1, respectively, in wild-type (WT), *Arrb1*$^{-/-}$ and *Arrb2*$^{-/-}$ mice. However, LPS-induced neuron loss and microglia activation were significantly alleviated in *Arrb1*$^{-/-}$ mice, but exacerbated in *Arrb2*$^{-/-}$ mice, as compared with those in WT mice (Fig. 2a-h).

We next determined the effects of ARRB knockout on neuroinflammation by measuring the expression of inflammatory markers in the mouse midbrain. All pro-inflammatory markers tested, including *Il6, Il1b, Tnf*

and *Nos2* genes and inducible nitric-oxide synthase (iNOS, encoded by *Nos2*), were significantly decreased, whereas anti-inflammatory markers, including *Arg1, Ym-1* and *Mrc1* genes and CD206 (encoded by *Mrc1*), were increased in *Arrb1*$^{-/-}$ mice after LPS challenge, as compared with those in WT mice. In marked contrast, the pro-inflammatory markers were enhanced and the anti-inflammatory markers were reduced (Fig. 2i-m) in *Arrb2*$^{-/-}$ mice as compared with those in WT mice. Similar to the results observed in LPS-induced PD models, knockout of ARRB1 and ARRB2 produced opposite effects on DA neuron loss, microglia activation, and neuroinflammation in MPTP-induced PD mouse models *in vivo* (Additional file 3: Figure S3).

Effects of ARRB depletion on microglia-induced DA neuron damage.

To define if the effects of ARRBs on DA neuron loss were indeed caused by their actions on microglia activation as observed in the PD mouse models *in vivo*, we measured the effects of conditioned medium (CM) collected from microglia with or without LPS + IFN-γ treatment on DA neuron apoptosis, death and survival *in vitro*. The CM from microglia treated with LPS + IFN-γ strongly lowered the expression of anti-apoptotic Bcl-2, but elevated the expression of pro-apoptotic Bax in the neurons (Fig. 3a-d) and reduced the viability of the neurons (Fig. 3e-f). The neurons exhibited apoptotic features, including chromatin condensation and nuclear fragmentation (Fig. 3g-j). The CM from microglia treated with LPS + IFN-γ also decreased the expression of TH (Fig. 3a-d) and shrunk the length of DA neuron axons (Fig. 3k-n). All of these deleterious effects on the DA neurons were clearly mitigated by the CM from ARRB1 siRNA-treated microglia, but intensified by the CM from ARRB2 knockout microglia (Fig. 3). These results indicate that ARRB1 knockout can rescue, whereas ARRB2 depletion further amplify, the DA neuron damage induced by microglia inflammatory responses.

Functions of ARRBs in inflammatory response of primary microglia and macrophages.

The gain- and loss-of-function approaches were used to further study the roles of ARRBs in microglia-mediated inflammation in response to LPS plus IFN-γ stimulation. In the gain-of-function studies, ARRB1 overexpression (Additional file 3: Figure S4a-b) significantly promoted, whereas ARRB2 overexpression (Additional file 3: Figure S4c-d) reduced, the expression of pro-inflammatory marker genes (*TNF-α*, *IL-6*, *IL-1β* and *iNOS*) in microglia (Fig. 4a-b). In the loss-of-function studies, siRNA-mediated ARRB1 knockdown (Additional file 3: Figure S4e-f) significantly inhibited (Fig. 4c), whereas ARRB2 knockout raised, the expression of the pro-inflammatory markers (Fig. 4d).

As microglia and macrophages have similar properties in mediating inflammation [43–45], bone marrow-derived macrophages (BMDMs) were used to confirm the functions of ARRBs in microglia-mediated inflammation. Similar to the results observed in microglia, siRNA-mediated ARRB1 knockdown markedly lowered the expression of pro-inflammatory marker genes and iNOS in BMDMs after LPS plus IFN-γ stimulation (Fig. 5a, c-d), whereas either siRNA-mediated knockdown (Additional file 3: Figure S5a-b) or knockout of ARRB2 enhanced the expression of pro-inflammatory markers (Fig. 5b, e-f, Additional file 3: Figure S5c). Furthermore, ARRB1 knockdown decreased, whereas ARRB2 knockout increased, the release

of pro-inflammatory cytokines (IL-6, IL-1β and TNF-α) as measured by ELISA (Fig. 5g-h). Immunofluorescent imaging showed that ARRB1 siRNA attenuated the expression of CD16, a pro-inflammatory marker, in BMDMs upon stimulation with LPS plus IFN-γ (Fig. 5i-j). In contrast, ARRB2 depletion enhanced CD16 expression (Fig. 5k-l) in BMDMs. These data demonstrate that ARRB1 and ARRB2 expression levels may directly control the inflammatory responses in a contrary manner in microglia and macrophages

Roles of ARRBs in the activation of inflammatory pathways and their interaction with p65.

As activation of the NF-κB and STAT1 pathways plays an essential role in inflammatory responses [46–48], we determined if ARRBs could regulate these two pathways. siRNA-mediated ARRB1 knockdown significantly inhibited, whereas ARRB2 knockdown stimulated, the activation of inhibitor of NF-κB (IκB) kinase β (IKKβ) and p65 in the NF-κB pathway in BMDMs treated with LPS plus IFN-γ (Fig. 6a-h). STAT1 activation was also impaired by ARRB1 knockdown (Fig. 6i-j), but strengthened by ARRB2 knockdown (Fig. 6k-l) in BMDMs. These results suggest that ARRB1 and ARRB2 may differentially regulate the activation of the NF-κB and STAT1 pathways.

ARRBs have been shown to interact with three molecules, IκBα, IKKα, and IKKβ [49–51] in the NF-κB pathway. To determine if ARRBs could bind other molecules in this pathway, we measured their interaction with p65. ARRB1 and ARRB2 were found to robustly interact with p65 in co-IP assays. More interestingly, both interactions fully depended on inflammatory stimulation (Fig. 6m-n). Furthermore, siRNA-mediated knockdown of one ARRB isoform clearly potentiated the interaction of the other isoform with p65 (Fig. 6o-p). These results suggest that two ARRBs physically associate with p65 likely in a competitive fashion.

Nprl3 as a novel effector of ARRBs in microglia.

To identify the effectors acting downstream of ARRBs, RNA sequencing (RNA-seq) was performed to compare genome-wide transcriptional profiles in microglia from WT or *Arrb2*$^{-/-}$ mice in response to inflammatory stimulation (Additional file 3: Figure S6a). This strategy identified 130 genes upregulated and 56 genes downregulated in *Arrb2*$^{-/-}$ mice, as compared with WT mice (Additional file 3: Figure S6b). Analysis of the enriched biological processes (BP) showed that upregulated genes were related to positive regulation of immune responses, whereas downregulated genes associated with negative regulation (Additional file 3: Figure S6b). Analysis of the enriched KEGG pathways also showed that upregulated genes were linked to inflammatory and immunological responses (Additional file 3: Figure S6c). Consistent with our results above (Fig. 3b), the RNA-seq data showed that the expression of pro-inflammatory genes, including *Il1b, Tnf*, *Il6* and *Nos2*, was increased in *Arrb2*$^{-/-}$ mice as compared with WT mice (Fig. 7a).

Based on the RNA-seq data, 15 inflammation-related genes were clearly changed in *Arrb2*$^{-/-}$ mice as compared with WT mice (Fig. 7b), and 11 of them (*Il12rb1, Lpar1, Gpat3, P2ry14, S100a1, Pttg1, Nes, Tmem100, CD5l, Tom1l1* and *Nprl3*) were confirmed by RT-PCR (Fig. 7c).

To determine if ARRB1 could alter the expression of these 11 gens, we measured the effects of siRNA-mediated knockdown of ARRB1 in microglia. Among these 11 genes, 3 genes, including *Il12rb1, Lpar1* and *Nprl3* which were increased in microglia from *Arrb2*$^{-/-}$ mice, were decreased in ARRB1-depleted microglia (Fig. 7d) as measured by RT-PCR.

Il12rb1 and Lpar1 are receptors for IL-12 and lysophosphatidic acid (LPA), respectively, and both are well known to regulate inflammatory responses [52–55]. The functions of Nprl3, however, are poorly studied and thus, it was selected to be studied in microglia activation. As our data demonstrated that Nprl3 was downregulated in *Arrb1*$^{-/-}$ mice and upregulated in *Arrb2*$^{-/-}$ mice, we determined the effects of Nprl3 overexpression in ARRB1-depleted microglia and the effects of Nprl3 knockdown in ARRB2-depleted microglia on inflammatory responses. Transient expression of Nprl3 (Additional file 3: Figure S7a-b) enhanced the expression of pro-inflammatory marker genes (*Il6, Il1b, Tnf* and *Nos2*), as well as the activation of p65 and STAT1 in ARRB1-knockout microglia, as compared with cells transfected with control vectors (Fig. 8a, c-f). siRNA-mediated Nprl3 knockdown (Additional file 3: Figure S7c-d) inhibited the expression of pro-inflammatory marker genes and the activation of p65 and STAT1 in ARRB2-knockout microglia (Fig. 8b, g-j). These results suggest that Nprl3 is a novel effector, acting downstream of both ARRBs and mediating their functions in microglia inflammatory responses and activation of the NF-κB and STAT1 pathways.

Discussion

In this study, we have demonstrated that ARRB1 and ARRB2, two closely related ARRBs, display functional antagonism in the pathogenesis of PD (Fig. 9) which is mediated through their distinct actions on microglia inflammatory responses. We first found that the expression of ARRB1 and ARRB2 was adversely regulated in the SNc and microglia of PD mouse models. We then used *Arrb1*$^{-/-}$ and *Arrb2*$^{-/-}$ mice to demonstrate that genetic ablation of ARRB1 significantly ameliorated, whereas knockout of ARRB2 exaggerated, DA neuron degeneration, microglia activation, and neuroinflammation in two PD mouse models *in vivo*. The opposing functions of ARRB1 and ARRB2 were also observed in DA neuron damage, microglia-mediated inflammation, and the activation of inflammatory signaling pathways in the gain- and loss-of-function studies using primary cell cultures *in vitro*. These data demonstrate that the expression of individual ARRBs as well as their expression ratio, specifically in microglia, is a crucial tipping point to control microglia inflammatory responses which in turn affect DA neuron degeneration and eventually the development of PD (Fig. 9).

We have also identified that Nprl3 is a novel effector, acting downstream of ARRBs and mediating their opposite effects on microglia inflammation. Nprl3 is a component of the gap activity towards rags 1 (GATOR1) complex and regulates mTOR complex 1 (mTORC1) signaling; it is associated with the pathogenesis of epilepsy and cancer [56–58]. However, its physiological functions remain largely unknown. In the current study, Nprl3 was identified as an effector of ARRBs by RNA-seq analysis of genome-wide transcriptional profiles, which was further confirmed by its ability to control the functions of ARRBs in microglia-mediated inflammatory responses, including the expression of pro-inflammatory

factors and activation of the NF-κB and STAT1 pathways. It is worth noting that ARRB1 and ARRB2 competitively interact with p65 and the interaction is completely dependent on inflammatory stimulation, suggestive of p65 activation-dependent interaction. Previous studies have revealed that the effects of ARRBs on the activation of the NF-κB pathway depend on stimuli and cell types studied [28, 59] and the underlying mechanisms may involve direct interaction with IκBα, IKKα, and IKKβ [49–51]. Our data not only suggest a novel mechanism by which ARRBs activate the NF-κB pathway, but also imply distinct functions of ARRBs in PD being attributable to their different abilities to interact with p65.

Our data presented in this study have demonstrated that, to the best of our knowledge, ARRB1 and ARRB2 are the only and first pair of closely related isoforms which produce completely opposing functions in both *in vivo* and *in vitro* models of PD. Based on these data, we can conclude that the normal function of ARRB1 in microglia is stimulatory, whereas the normal function of ARRB2 is inhibitory, with respective to the expression of Nprl3, the activation of the STAT1 and NFκB pathways, inflammatory responses, and pathologic progression of PD (Fig. 9). As such, these data imply a potential therapeutic intervention, using genetic and/or pharmacological approaches to inhibit ARRB1 function and enhance ARRB2 function simultaneously,

It is interesting to note that distinct expression and function of ARRB1 and ARRB2 have been observed in other animal and cellular settings [59, 60]. For example, in an experimental autoimmune encephalomyelitis (EAE) mouse model, ARRB1 knockout alleviates disease phenotypes [32], whereas ARRB2 deficiency exacerbates EAE symptoms [33]. In a cellular model, ARRB1 downregulation increases, whereas ARRB2 depletion reduces, angiotensin II receptor-mediated activation of extracellular signal-regulated kinases 1 and 2 [61, 62]. Similar to the results observed in this study, both ARRB1 and ARRB2 interact with NLRP3 inflammasome, but they produce functionally contrary effects on the inflammasome activation [63, 64]. These data, together with our current study, demonstrate the extreme complexity of ARRB-mediated functions under different physiological and pathological conditions.

Conclusion

This study reveals for the first time important, but opposite, roles played by ARRB1 and ARRB2 in the microglia-mediated inflammation and pathogenesis of PD. Our results provide novel insights into the understanding of the functional divergence of ARRBs in PD and may aid in the development of drugs for the treatment of PD.

Abbreviations

PD: Parkinson’s disease; AD: Alzheimer’s disease; DA: dopaminergic; SNc: substantia nigra pars compacta; TNFα: tumor necrosis factor α; IL: interleukin; IFN-γ: interferon-γ; ARRB: β-Arrestin; ARRB2: β-arrestin2; ARRB1: β-arrestin1; GPCR: G protein-coupled receptor; TH: tyrosine hydroxylase; NLRP3: NOD-like receptor protein-3; Nprl3: nitrogen permease regulator-like 3; NF-κB: nuclear factor (NF)-κB; STAT: signal transducers and activators of transcription; LPS: lipopolysaccharide; MPTP: 1-methyl-4-phenyl-1, 2,

3, 6-tetrahydropyridine; ionized calcium binding adapter molecule (Iba)-1: Iba1; GFAP: glial fibrillary acidic protein; Arrb1$^{-/-}$: β-Arrestin1 knockout; Arrb2$^{-/-}$: β-Arrestin2 knockout; PLL: poly-L-lysine; BSA: bovine serum albumin; FBS: fetal bovine serum; GM-CSF: granulocyte-macrophage colony stimulating factor; WT: wild type; PFA: Paraformaldehyde; Scramble: negative control; iNOS: inducible nitric-oxide synthase; CM: conditioned medium; Bcl-2: B-cell lymphoma (Bcl)-2; Bax: Bcl2-associated X protein; BMDM: bone marrow-derived macrophage; IKK: inhibitor of NF-κB (IκB) kinase; Co-IP: Co-immunoprecipitation; RNA-seq: RNA sequencing; BP: biological processes; KEGG: kyoto encyclopedia of genes and genomes; GATOR1: GAP Activity Towards Rags 1; mTORC1: mTOR complex 1; EAE: experimental autoimmune encephalomyelitis

Declarations

Ethics approval

All animal tests were carried out in accordance with the US National Institutes of Health (NIH) Guide for the Care and Use of Laboratory. All experimental procedures were approved by the Institutional Animal Care and Use Committee (IACUC) of the Nanjing Medical University Experimental Animal Department (IACUC-1811049). This article does not contain any studies with human participants performed by any of the authors.

Consent for publication

All authors read and approved the final manuscript

Availability of data and materials

The datasets supporting the conclusions of this article are included within the supplementary information available at *Molecular Neurodegeneration* website.

Competing interests

The authors have declared that no Competing interests exist.

Funding

The work reported herein was supported by the grants from the National Natural Science Foundation of China (No. 81630099, 81703488), the Drug Innovation Major Project (No. 2018ZX09711001-003-007), the Natural Science Foundation of the Basic Research Program of Jiangsu Province (No. BK20171061), and the National Institutes of Health (R01GM118915 and R35GM136397).

Author contributions

In this study, YQF, QLJ, ML, JHD and GH conceived and designed the experiments. YQF, QLJ, SSL, HZ, XD, RX, MMC, NSS and MMS carried out the experiments. YQF, QLJ, GW, ML and GH analyzed the data and

wrote the paper. GH critically reviewed and edited the work. All authors approved the final version of the manuscript.

Acknowledgements

We would like to acknowledge Drs. Gang Pei and Lan Ma for providing *Arrb2*$^{-/-}$ mice and ARRB2 plasmid, respectively.

Authors' information

[1]Jiangsu Key Laboratory of Neurodegeneration, Department of Pharmacology, Nanjing Medical University, 818 Tianyuan East Road, Nanjing, Jiangsu 211166, China

[2]Department of Pharmacology, Nanjing University of Chinese Medicine, 138 Xianlin Avenue, Nanjing, Jiangsu 210023, China

[3]Department of Pharmacology and Toxicology, Medical College of Georgia, Augusta University, 1459 Laney Walker Blvd., Augusta, GA 30912, USA

References

1. Poewe W, Seppi K, Tanner CM, Halliday GM, Brundin P, Volkmann J, Schrag AE, Lang AE. Parkinson disease. Nat Rev Dis Primers. 2017;3:17013.
2. Homayoun H. Parkinson Disease. Ann Intern Med. 2018;169(5):Itc33–48.
3. Zeng XS, Geng WS, Jia JJ, Chen L, Zhang PP. Cellular and Molecular Basis of Neurodegeneration in Parkinson Disease. Front Aging Neurosci. 2018;10:109.
4. Wang Q, Liu Y, Zhou J. Neuroinflammation in Parkinson's disease and its potential as therapeutic target. Transl Neurodegener. 2015;4:19.
5. Bachiller S, Jimenez-Ferrer I, Paulus A, Yang Y, Swanberg M, Deierborg T, Boza-Serrano A. Microglia in Neurological Diseases: A Road Map to Brain-Disease Dependent-Inflammatory Response. Front Cell Neurosci. 2018;12:488.
6. Prinz M, Jung S, Priller J. Microglia Biology: One Century of Evolving Concepts. Cell. 2019;179(2):292–311.
7. Hamza TH, Zabetian CP, Tenesa A, Laederach A, Montimurro J, Yearout D, Kay DM, Doheny KF, Paschall J, Pugh E, et al. Common genetic variation in the HLA region is associated with late-onset sporadic Parkinson's disease. Nat Genet. 2010;42(9):781–5.
8. Rayaprolu S, Mullen B, Baker M, Lynch T, Finger E, Seeley WW, Hatanpaa KJ, Lomen-Hoerth C, Kertesz A, Bigio EH, et al. TREM2 in neurodegeneration: evidence for association of the p.R47H variant with frontotemporal dementia and Parkinson's disease. Molecular neurodegeneration. 2013;8:19.

9. Sawada M, Imamura K, Nagatsu T. Role of cytokines in inflammatory process in Parkinson's disease. J Neural Transm Suppl 2006(70):373–381.
10. Chung YC, Baek JY, Kim SR, Ko HW, Bok E, Shin WH, Won SY, Jin BK. Capsaicin prevents degeneration of dopamine neurons by inhibiting glial activation and oxidative stress in the MPTP model of Parkinson's disease. Exp Mol Med. 2017;49(3):e298.
11. Imamura K, Hishikawa N, Sawada M, Nagatsu T, Yoshida M, Hashizume Y. Distribution of major histocompatibility complex class II-positive microglia and cytokine profile of Parkinson's disease brains. Acta Neuropathol. 2003;106(6):518–26.
12. Wu XF, Block ML, Zhang W, Qin L, Wilson B, Zhang WQ, Veronesi B, Hong JS. The role of microglia in paraquat-induced dopaminergic neurotoxicity. Antioxid Redox Signal. 2005;7(5–6):654–61.
13. Su X, Federoff HJ, Maguire-Zeiss KA. Mutant alpha-synuclein overexpression mediates early proinflammatory activity. Neurotox Res. 2009;16(3):238–54.
14. Bartels AL, Willemsen AT, Doorduin J, de Vries EF, Dierckx RA, Leenders KL. [11C]-PK11195 PET: quantification of neuroinflammation and a monitor of anti-inflammatory treatment in Parkinson's disease? Parkinsonism Relat Disord. 2010;16(1):57–9.
15. Sanchez-Guajardo V, Febbraro F, Kirik D, Romero-Ramos M. Microglia acquire distinct activation profiles depending on the degree of alpha-synuclein neuropathology in a rAAV based model of Parkinson's disease. PLoS One. 2010;5(1):e8784.
16. Bond RA, Lucero Garcia-Rojas EY, Hegde A, Walker JKL. Therapeutic Potential of Targeting β-Arrestin. Front Pharmacol. 2019;10:124.
17. Gurevich VV, Gurevich EV. GPCR Signaling Regulation: The Role of GRKs and Arrestins. Front Pharmacol. 2019;10:125.
18. Cottingham C, Li X, Wang Q. Noradrenergic antidepressant responses to desipramine in vivo are reciprocally regulated by arrestin3 and spinophilin. Neuropharmacology. 2012;62(7):2354–62.
19. Kang DS, Tian X, Benovic JL. Role of beta-arrestins and arrestin domain-containing proteins in G protein-coupled receptor trafficking. Curr Opin Cell Biol. 2014;27:63–71.
20. Shi Q, Li M, Mika D, Fu Q, Kim S, Phan J, Shen A, Vandecasteele G, Xiang YK. Heterologous desensitization of cardiac beta-adrenergic signal via hormone-induced betaAR/arrestin/PDE4 complexes. Cardiovasc Res. 2017;113(6):656–70.
21. Schmid CL, Bohn LM. Physiological and pharmacological implications of beta-arrestin regulation. Pharmacol Ther. 2009;121(3):285–93.
22. Peterson YK, Luttrell LM. The Diverse Roles of Arrestin Scaffolds in G Protein-Coupled Receptor Signaling. Pharmacol Rev. 2017;69(3):256–97.
23. Alekhina O, Marchese A. beta-Arrestin1 and Signal-transducing Adaptor Molecule 1 (STAM1) Cooperate to Promote Focal Adhesion Kinase Autophosphorylation and Chemotaxis via the Chemokine Receptor CXCR4. J Biol Chem. 2016;291(50):26083–97.

24. Weinberg ZY, Zajac AS, Phan T, Shiwarski DJ, Puthenveedu MA. Sequence-Specific Regulation of Endocytic Lifetimes Modulates Arrestin-Mediated Signaling at the micro Opioid Receptor. Mol Pharmacol. 2017;91(4):416–27.
25. Shenoy SK, Lefkowitz RJ. beta-Arrestin-mediated receptor trafficking and signal transduction. Trends Pharmacol Sci. 2011;32(9):521–33.
26. Parameswaran N, Pao CS, Leonhard KS, Kang DS, Kratz M, Ley SC, Benovic JL. Arrestin-2 and G protein-coupled receptor kinase 5 interact with NFkappaB1 p105 and negatively regulate lipopolysaccharide-stimulated ERK1/2 activation in macrophages. J Biol Chem. 2006;281(45):34159–70.
27. Fan H, Luttrell LM, Tempel GE, Senn JJ, Halushka PV, Cook JA. Beta-arrestins 1 and 2 differentially regulate LPS-induced signaling and pro-inflammatory gene expression. Mol Immunol. 2007;44(12):3092–9.
28. Ahmadzai MM, Broadbent D, Occhiuto C, Yang C, Das R, Subramanian H. Canonical and Noncanonical Signaling Roles of beta-Arrestins in Inflammation and Immunity. Advances in immunology. 2017;136:279–313.
29. Wang P, Xu TY, Wei K, Guan YF, Wang X, Xu H, Su DF, Pei G, Miao CY. ARRB1/beta-arrestin-1 mediates neuroprotection through coordination of BECN1-dependent autophagy in cerebral ischemia. Autophagy. 2014;10(9):1535–48.
30. Liu X, Zhao X, Zeng X, Bossers K, Swaab DF, Zhao J, Pei G. beta-arrestin1 regulates gamma-secretase complex assembly and modulates amyloid-beta pathology. Cell Res. 2013;23(3):351–65.
31. Thathiah A, Horre K, Snellinx A, Vandewyer E, Huang Y, Ciesielska M, De Kloe G, Munck S. De Strooper B: beta-arrestin 2 regulates Abeta generation and gamma-secretase activity in Alzheimer's disease. Nat Med. 2013;19(1):43–9.
32. Shi Y, Feng Y, Kang J, Liu C, Li Z, Li D, Cao W, Qiu J, Guo Z, Bi E, et al. Critical regulation of CD4 + T cell survival and autoimmunity by beta-arrestin 1. Nat Immunol. 2007;8(8):817–24.
33. Zhang Y, Liu C, Wei B, Pei G. Loss of beta-arrestin 2 exacerbates experimental autoimmune encephalomyelitis with reduced number of Foxp3 + CD4 + regulatory T cells. Immunology. 2013;140(4):430–40.
34. Feng X, Wu CY, Burton FH, Loh HH, Wei LN. beta-arrestin protects neurons by mediating endogenous opioid arrest of inflammatory microglia. Cell Death Differ. 2014;21(3):397–406.
35. Urs NM, Bido S, Peterson SM, Daigle TL, Bass CE, Gainetdinov RR, Bezard E, Caron MG. Targeting beta-arrestin2 in the treatment of L-DOPA-induced dyskinesia in Parkinson's disease. Proc Natl Acad Sci U S A. 2015;112(19):E2517–26.
36. Zhu J, Hu Z, Han X, Wang D, Jiang Q, Ding J, Xiao M, Wang C, Lu M, Hu G. Dopamine D2 receptor restricts astrocytic NLRP3 inflammasome activation via enhancing the interaction of beta-arrestin2 and NLRP3. Cell Death Differ. 2018;25(11):2037–49.
37. Han X, Sun S, Sun Y, Song Q, Zhu J, Song N, Chen M, Sun T, Xia M, Ding J, et al: Small molecule-driven NLRP3 inflammation inhibition via interplay between ubiquitination and autophagy:

implications for Parkinson disease. Autophagy 2019:1–22.

38. Fang Y, Wang J, Yao L, Li C, Wang J, Liu Y, Tao X, Sun H, Liao H. The adhesion and migration of microglia to beta-amyloid (Abeta) is decreased with aging and inhibited by Nogo/NgR pathway. J Neuroinflammation. 2018;15(1):210.
39. Song N, Fang Y, Sun X, Jiang Q, Song C, Chen M, Ding J, Lu M, Hu G. Salmeterol, agonist of beta2-aderenergic receptor, prevents systemic inflammation via inhibiting NLRP3 inflammasome. Biochem Pharmacol. 2018;150:245–55.
40. Hu ZL, Sun T, Lu M, Ding JH, Du RH, Hu G. Kir6.1/K-ATP channel on astrocytes protects against dopaminergic neurodegeneration in the MPTP mouse model of Parkinson's disease via promoting mitophagy. Brain Behav Immun. 2019;81:509–22.
41. Qiao C, Zhang Q, Jiang Q, Zhang T, Chen M, Fan Y, Ding J, Lu M, Hu G. Inhibition of the hepatic Nlrp3 protects dopaminergic neurons via attenuating systemic inflammation in a MPTP/p mouse model of Parkinson's disease. J Neuroinflammation. 2018;15(1):193.
42. Duty S, Jenner P. Animal models of Parkinson's disease: a source of novel treatments and clues to the cause of the disease. Br J Pharmacol. 2011;164(4):1357–91.
43. Xiong XY, Liu L, Yang QW. Functions and mechanisms of microglia/macrophages in neuroinflammation and neurogenesis after stroke. Prog Neurobiol. 2016;142:23–44.
44. Wang J. Preclinical and clinical research on inflammation after intracerebral hemorrhage. Prog Neurobiol. 2010;92(4):463–77.
45. Franco R, Fernandez-Suarez D. Alternatively activated microglia and macrophages in the central nervous system. Prog Neurobiol. 2015;131:65–86.
46. Hou L, Sun F, Huang R, Sun W, Zhang D, Wang Q. Inhibition of NADPH oxidase by apocynin prevents learning and memory deficits in a mouse Parkinson's disease model. Redox Biol. 2019;22:101134.
47. Kelly R, Joers V, Tansey MG, McKernan DP, Dowd E. Microglial Phenotypes and Their Relationship to the Cannabinoid System: Therapeutic Implications for Parkinson's Disease. Molecules (Basel, Switzerland) 2020, 25(3).
48. Rangaraju S, Dammer EB, Raza SA, Rathakrishnan P, Xiao H, Gao T, Duong DM, Pennington MW, Lah JJ, Seyfried NT, et al. Identification and therapeutic modulation of a pro-inflammatory subset of disease-associated-microglia in Alzheimer's disease. Molecular neurodegeneration. 2018;13(1):24.
49. Freedman NJ, Shenoy SK. Regulation of inflammation by beta-arrestins: Not just receptor tales. Cellular signalling. 2018;41:41–5.
50. Gao H, Sun Y, Wu Y, Luan B, Wang Y, Qu B, Pei G. Identification of beta-arrestin2 as a G protein-coupled receptor-stimulated regulator of NF-kappaB pathways. Mol Cell. 2004;14(3):303–17.
51. Witherow DS, Garrison TR, Miller WE, Lefkowitz RJ. beta-Arrestin inhibits NF-kappaB activity by means of its interaction with the NF-kappaB inhibitor IkappaBalpha. Proc Natl Acad Sci U S A. 2004;101(23):8603–7.

52. Jana M, Mondal S, Jana A, Pahan K. Interleukin-12 (IL-12), but not IL-23, induces the expression of IL-7 in microglia and macrophages: implications for multiple sclerosis. Immunology. 2014;141(4):549–63.
53. Jana M, Dasgupta S, Pal U, Pahan K. IL-12 p40 homodimer, the so-called biologically inactive molecule, induces nitric oxide synthase in microglia via IL-12R beta 1. Glia. 2009;57(14):1553–65.
54. Jana M, Pahan K. IL-12 p40 homodimer, but not IL-12 p70, induces the expression of IL-6 in microglia and macrophages. Molecular immunology. 2009;46(5):773–83.
55. Plastira I, Bernhart E, Goeritzer M, DeVaney T, Reicher H, Hammer A, Lohberger B, Wintersperger A, Zucol B, Graier WF, et al. Lysophosphatidic acid via LPA-receptor 5/protein kinase D-dependent pathways induces a motile and pro-inflammatory microglial phenotype. J Neuroinflammation. 2017;14(1):253.
56. Ricos MG, Hodgson BL, Pippucci T, Saidin A, Ong YS, Heron SE, Licchetta L, Bisulli F, Bayly MA, Hughes J, et al. Mutations in the mammalian target of rapamycin pathway regulators NPRL2 and NPRL3 cause focal epilepsy. Ann Neurol. 2016;79(1):120–31.
57. Myers KA, Scheffer IE. DEPDC5 as a potential therapeutic target for epilepsy. Expert Opin Ther Targets. 2017;21(6):591–600.
58. Bar-Peled L, Chantranupong L, Cherniack AD, Chen WW, Ottina KA, Grabiner BC, Spear ED, Carter SL, Meyerson M, Sabatini DM. A Tumor suppressor complex with GAP activity for the Rag GTPases that signal amino acid sufficiency to mTORC1. Science. 2013;340(6136):1100–6.
59. Fan H. beta-Arrestins 1 and 2 are critical regulators of inflammation. Innate Immun. 2014;20(5):451–60.
60. Srivastava A, Gupta B, Gupta C, Shukla AK. Emerging Functional Divergence of beta-Arrestin Isoforms in GPCR Function. Trends Endocrinol Metab. 2015;26(11):628–42.
61. Ahn S, Wei H, Garrison TR, Lefkowitz RJ. Reciprocal regulation of angiotensin receptor-activated extracellular signal-regulated kinases by beta-arrestins 1 and 2. J Biol Chem. 2004;279(9):7807–11.
62. Wei H, Ahn S, Shenoy SK, Karnik SS, Hunyady L, Luttrell LM, Lefkowitz RJ. Independent beta-arrestin 2 and G protein-mediated pathways for angiotensin II activation of extracellular signal-regulated kinases 1 and 2. Proc Natl Acad Sci U S A. 2003;100(19):10782–7.
63. Yan Y, Jiang W, Spinetti T, Tardivel A, Castillo R, Bourquin C, Guarda G, Tian Z, Tschopp J, Zhou R. Omega-3 fatty acids prevent inflammation and metabolic disorder through inhibition of NLRP3 inflammasome activation. Immunity. 2013;38(6):1154–63.
64. Mao K, Chen S, Wang Y, Zeng Y, Ma Y, Hu Y, Zhang H, Sun S, Wu X, Meng G, et al. beta-arrestin1 is critical for the full activation of NLRP3 and NLRC4 inflammasomes. J Immunol. 2015;194(4):1867–73.

Supplemental Legends

Additional fie 3, Fig. S1, Related to Fig. 1 Expression of ARRB1 and ARRB2 in astrocytes (**a**) and neurons (**b**) in the SNc of LPS-induced PD model mice. Similar results were obtained in 3 separate experiments. Scale bars, 50 μm.

Additional fie 3, Fig. S2, related to Fig. 2 Expression of ARRB1 and ARRB2 in the midbrain of WT, *Arrb1*$^{-/-}$ and *Arrb2*$^{-/-}$ mice. **a** Representative blots. **b** Quantitative data shown in **a**. Quantitative data are mean ± s.e. (n = 3). NS, not significant.

Additional fie 3, Fig. S3, related to Fig. 2 Effects of ARRB1 or ARRB2 knockout on DA neuron death and microglia inflammation in MPTP-induced PD models. **a-h** Immunohistochemistry (**a**, **c**, **e and g**) and stereological counts (**b**, **d**, **f and h**) of TH^{+} DA neuron (**a-d**) and Iba-1^{+} microglia (**e-h**) in the SNc of MPTP-induced PD models. Scale bars, 200 μm (upper panels) or 40 μm (lower panels) in **a**, **c**, **e and g**. **i** mRNA levels of pro- and anti-inflammatory markers in the midbrain of PD mice. **j-m** Expression of CD206 and iNOS in the midbrain. Quantitative data are mean ± s.e. (n = 3-5). *P < 0.05, **P < 0.01, and ***P < 0.001.

Additional fie 3, Fig. S4, related to Fig. 4 Expression of ARRB1 and ARRB2 in microglia. **a-d** Expression of ARRB1 and ARRB2 in microglia after transfection with ARRB1 (**a-b**) or ARRB2 (**c-d**) for 24 h. **e-f** ARRB1 expression in microglia after transfection with different concentrations of ARRB1 siRNA or with scramble siRNA. Quantitative data are mean ± s.e. (n = 3). **P < 0.01 and ***P < 0.001.

Additional fie 3, Fig. S5, related to Fig. 5 Effects of ARRB2 knockdown on the expression of inflammatory markers in macrophages. **a-b** ARRB2 expression in BMDMs after transfection with 120 nM siRNA targeting ARRB2 for 48 h. **c** mRNA levels of inflammatory markers in ARRB2-knockdown BMDMs with or without LPS plus IFN-γ treatment for 6 h. Quantitative data are mean ± s.e. (n = 3). *P < 0.05, **P < 0.01 and ***P < 0.001.

Additional fie 3, Fig. S6, related to Fig. 7 Analysis of RNA-seq. **a** Heatmap of normalized read counts from WT or Arrb2$^{-/-}$ microglia treated with LPS plus IFN-γ for 6 h. The total RNA was sequenced on an Illumina HisSeq 4000. **b** A volcano plot of gene changes in microglia from *Arrb2*$^{-/-}$ mice as compared with those from WT mice after LPS plus IFN-γ treatment. Among 130 upregulated and 56 downregulated genes, the top 10 enriched BPs were determined. The intensity of the red color indicates the significance of BPs. **c** Enriched KEGG pathways found among the upregulated genes in microglia from *Arrb2*$^{-/-}$ mice as compared with WT mice.

Additional fie 3, Fig. S7, related to Fig. 8 Nprl3 expression in microglia after transfection with NPRL3 for 24 h (**a-b**) or Nprl3 siRNA for 48 h (**c-d**). Quantitative data are mean ± s.e. (n = 3). ***P < 0.001.

Additional fie 3, Fig. S8 Gel source data.

Figures

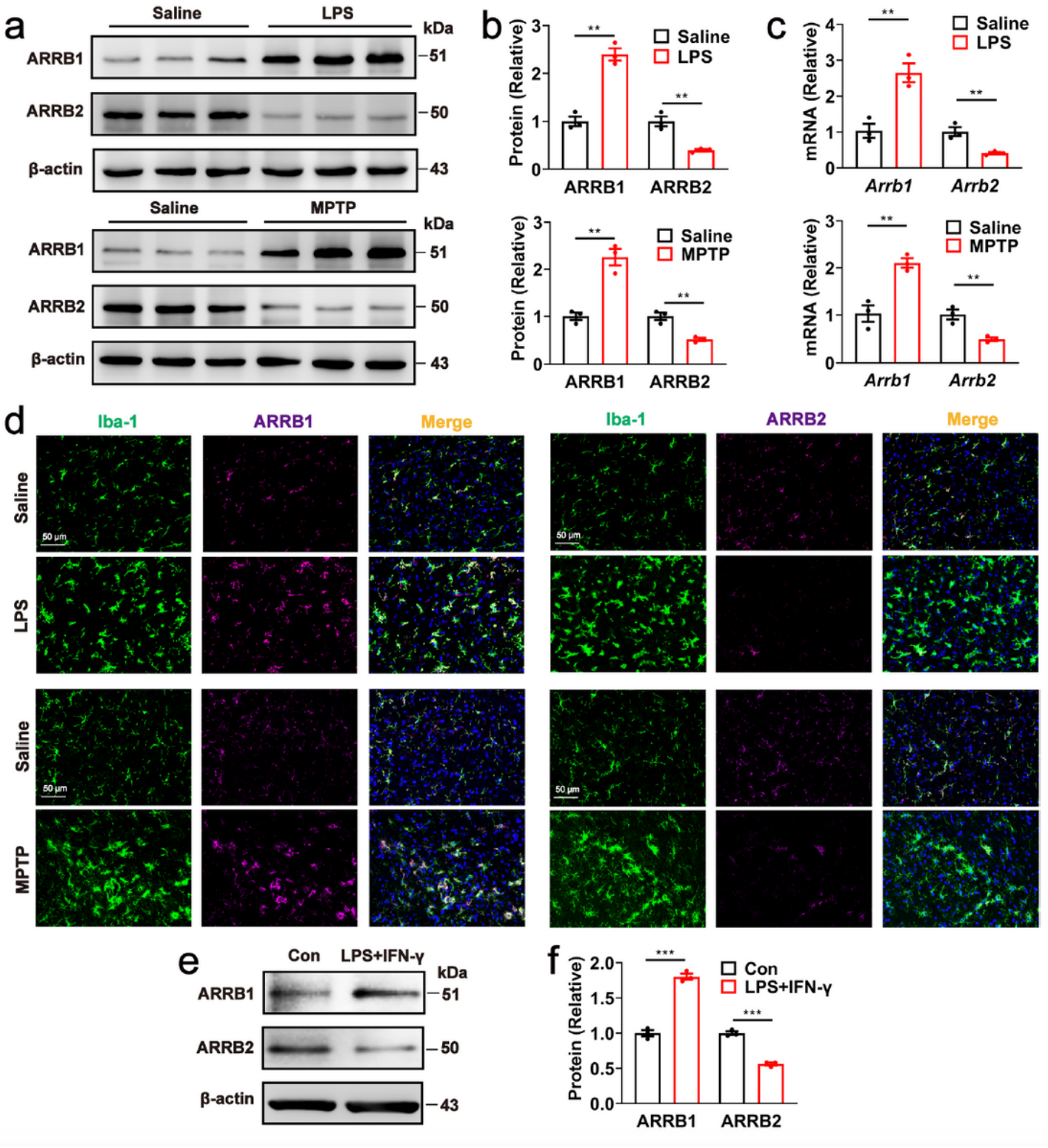

Figure 1

Expression of ARRB1 and ARRB2 in PD mouse models. a ARRB1 and ARRB2 expression in the SNc of LPS- and MPTP-induced PD mouse models. b Quantitative data shown in a. c mRNA of ARRB1 and ARRB2 in the SNc of PD mice measured by RT-PCR. d Expression of ARRB1 and ARRB2 in microglia (Iba-1) in the SNc of PD mouse models. Similar results were obtained in 3 separate experiments. e Expression

of ARRB1 and ARRB2 in primary microglia after LPS plus IFN-γ stimulation. f Quantitative data shown in e. Quantitative data are mean ± s.e. (n = 3). **P < 0.01 and ***P < 0.001. Scale bars, 50 μm.

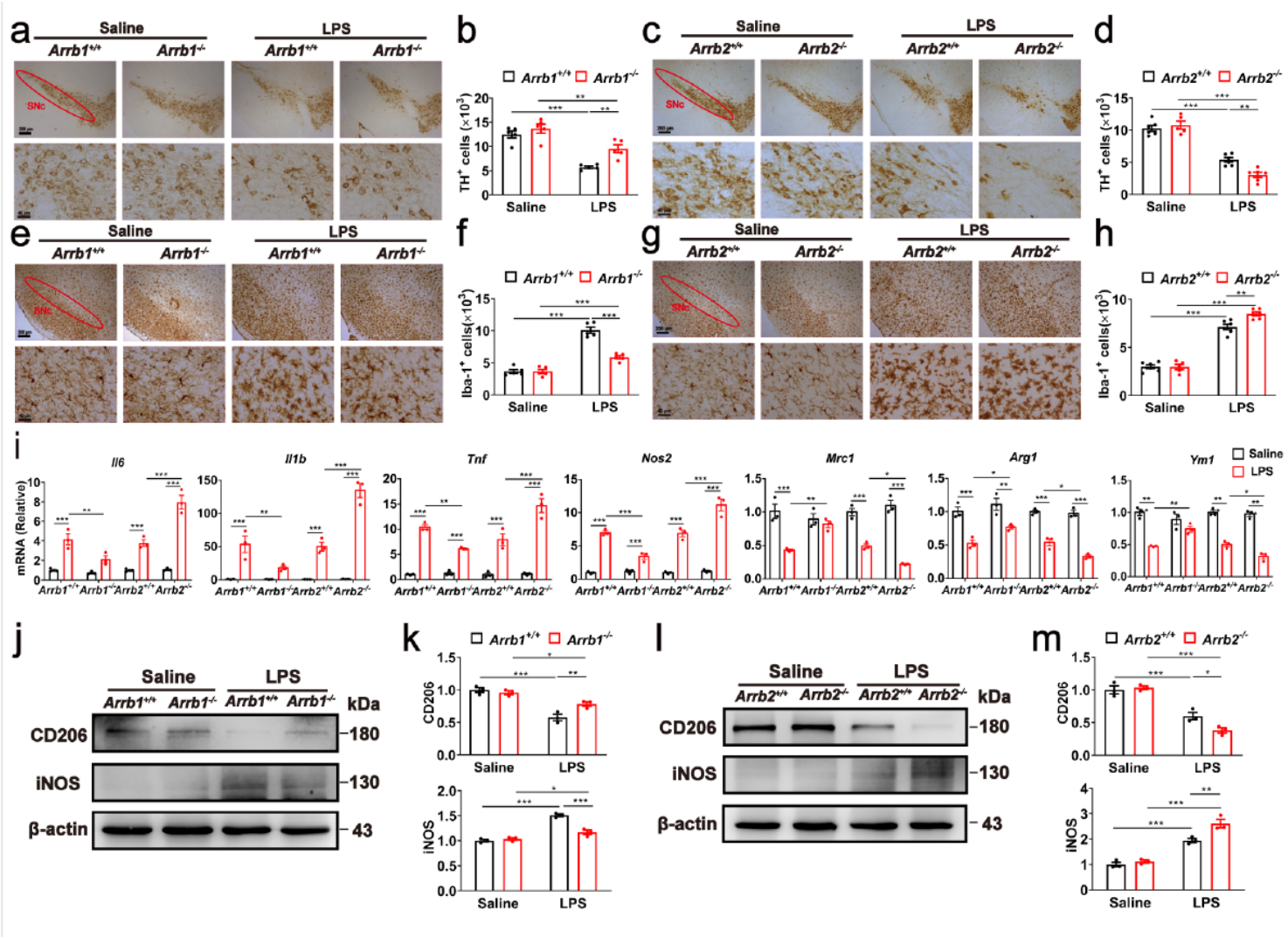

Figure 2

Effects of ARRB1 or ARRB2 knockout on neuron death and neuroinflammation in LPS-induced PD models. a-h Immunohistochemistry (a, c, e and g) and stereological counts (b, d, f and h) of TH+ DA neuron (a-d) and Iba-1+ microglia (e-h) in the SNc of LPS-induced PD models. Scale bars, 200 μm (upper panels) or 40 μm (lower panels) in a, c, e and g. i mRNA levels of pro- and anti-inflammatory markers in the midbrain of PD mice. j-m Expression of CD206 and iNOS in the midbrain. Quantitative data are mean ± s.e. (n = 3-5). *P < 0.05, **P < 0.01, and ***P < 0.001.

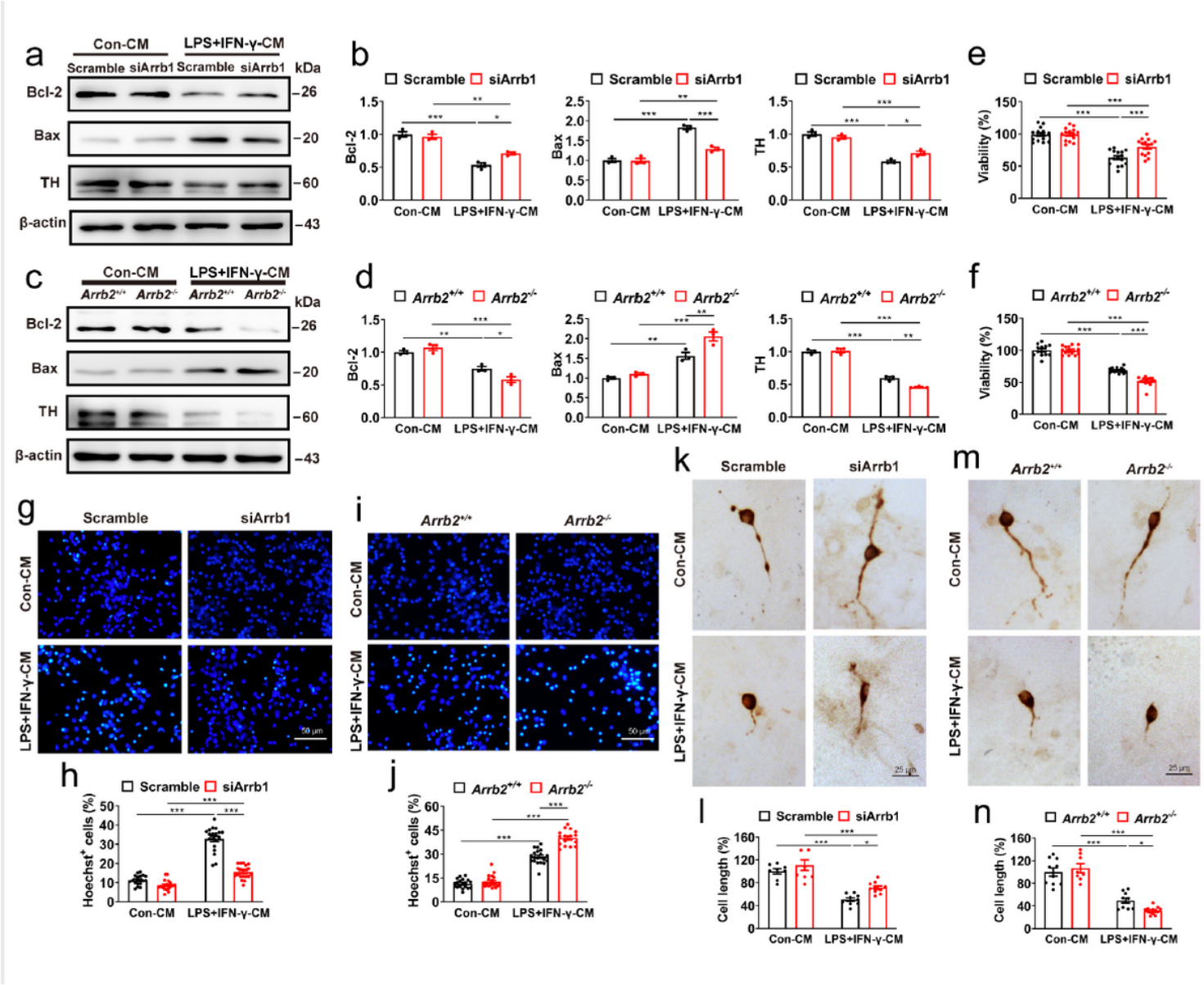

Figure 3

Effects of ARRB1 and ARRB2 depletion on microglia-induced DA neuron damage. a-d Expression of Bcl-2, Bax and TH in DA neurons treated with CMs of WT, siRNA-mediated ARRB1 knockdown or ARRB2-deficient microglia. e and f The viability of DA neurons. g-j l Nuclear morphology (g-i) and Hoechst-positive DA neurons (h-j). Scale bars, 50 μm. k-n Morphology of DA neurons (k-m) and TH+ cell neurite length (l-n). Scale bars, 25 μm. Quantitative data are mean ± s.e. (n = 3). *P < 0.05, **P < 0.01, and ***P < 0.001.

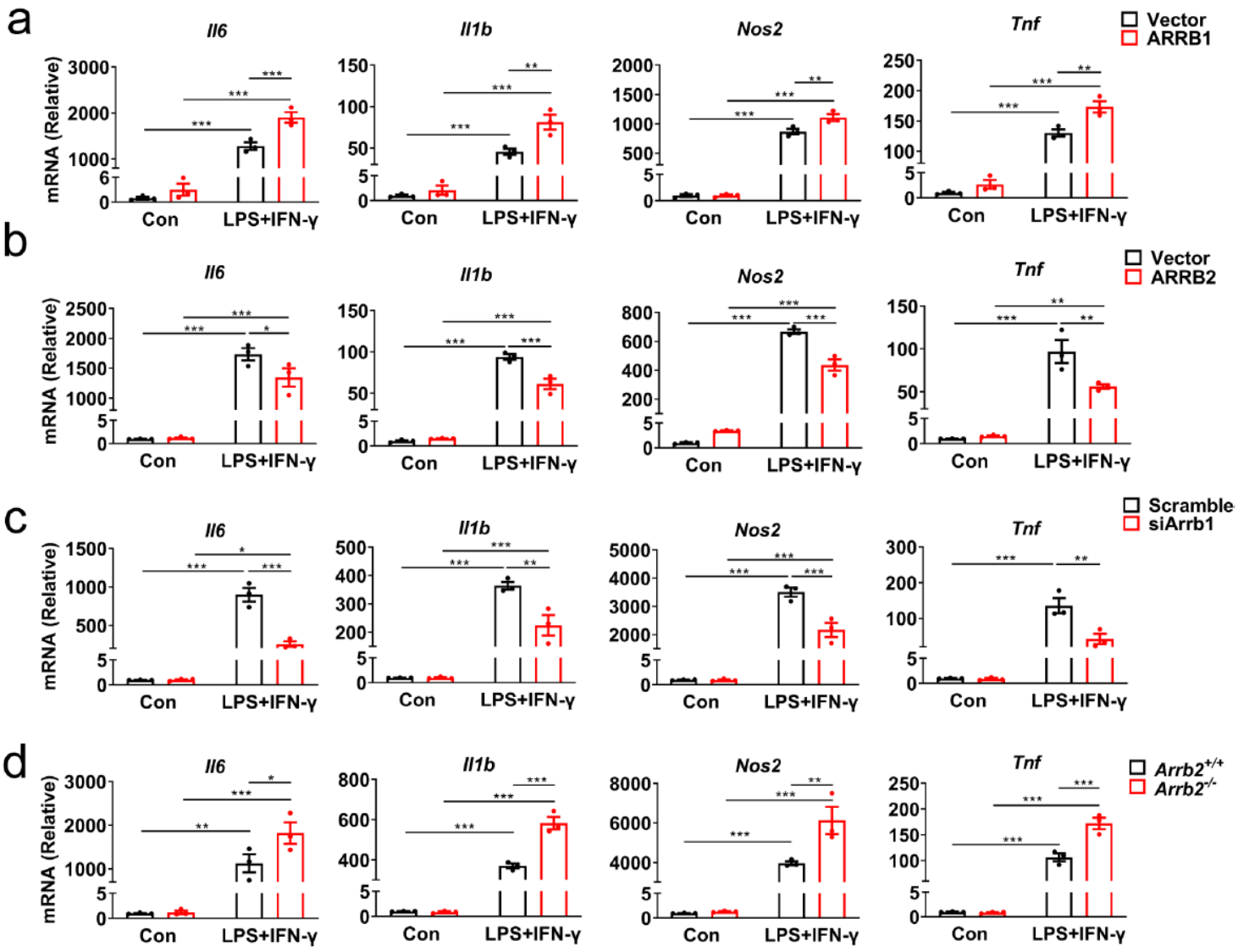

Figure 4

Effects of overexpression and depletion of ARRB1 or ARRB2 on microglia-mediated inflammation. a and b Levels of pro-inflammatory gene transcripts in microglia transfected with ARRB1 (a) or ARRB2 (b) after LPS plus IFN-γ stimulation for 6 h. c and d Pro-inflammatory gene expression in siRNA-mediated ARRB1 knockdown (c) and ARRB2 knockout (d) microglia. Quantitative data are mean ± s.e. (n = 3). **P < 0.01 and ***P < 0.001.

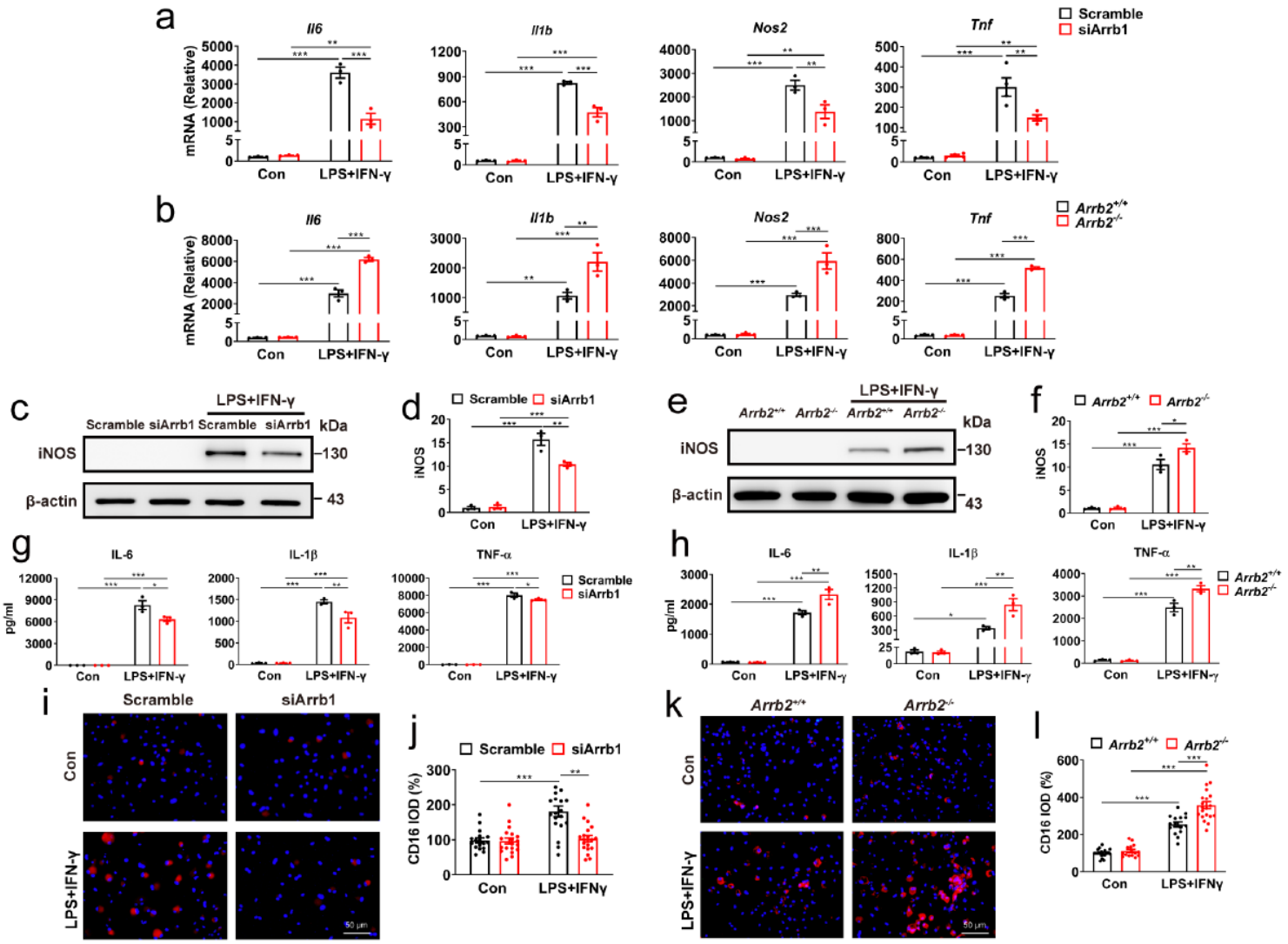

Figure 5

Effects of ARRB1 and ARRB2 depletion on inflammation in macrophages. a-b Levels of pro-inflammatory gene in siRNA-mediated ARRB1 knockdown and ARRB2 knockout BMDMs with or without LPS plus IFN-γ stimulation for 6 h. c-f iNOS expression in ARRB1 knockdown and ARRB2 knockout BMDMs after stimulation for 24 h. g-h IL-6, IL-1β and TNF-α expression in supernatants of ARRB1 knockdown and ARRB2 knockout BMDMs after stimulation for 24 h. i-l CD16 expression detected by immunofluorescence. Scale bars, 50 μm. Quantitative data are mean ± s.e. (n = 3). *P < 0.05, **P < 0.01, and ***P < 0.001.

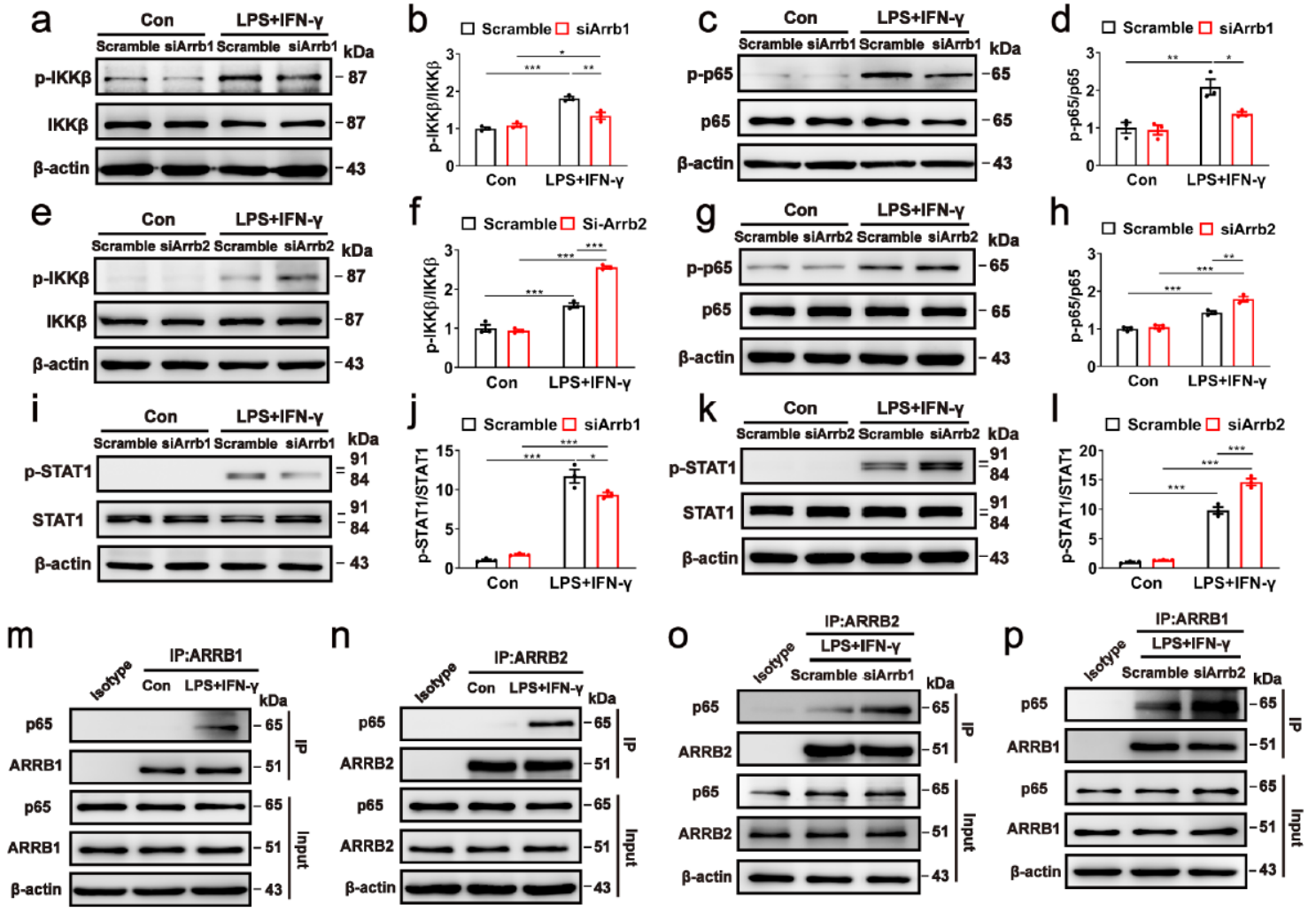

Figure 6

Effects of siRNA-mediated knockdown of ARRB1 or ARRB2 on activation of NF-κB and STAT1 pathways. a-l Activation of IKKβ (a, b, e and f), p65 (c, d, g and h) and STAT1 (i-l) in ARRB1 or ARRB2 siRNA-treated BMDMs with or without LPS plus IFN-γ stimulation for 2 h. m- n Interaction of ARRB1 or ARRB2 with p65. BMDMs were stimulated with LPS plus IFN-γ for 1 h and the cell lysates were immunoprecipitated with antibodies against ARRB1 (m) or ARRB2 (n). o Effect of ARRB1 knockdown on ARRB2 interaction with p65. p Effect of ARRB2 knockdown on ARRB1 interaction with p65. Blots shown in m-p are representatives of 3 independent experiments. Quantitative data are mean ± s.e. (n = 3). *P < 0.05, **P < 0.01, and ***P < 0.001.

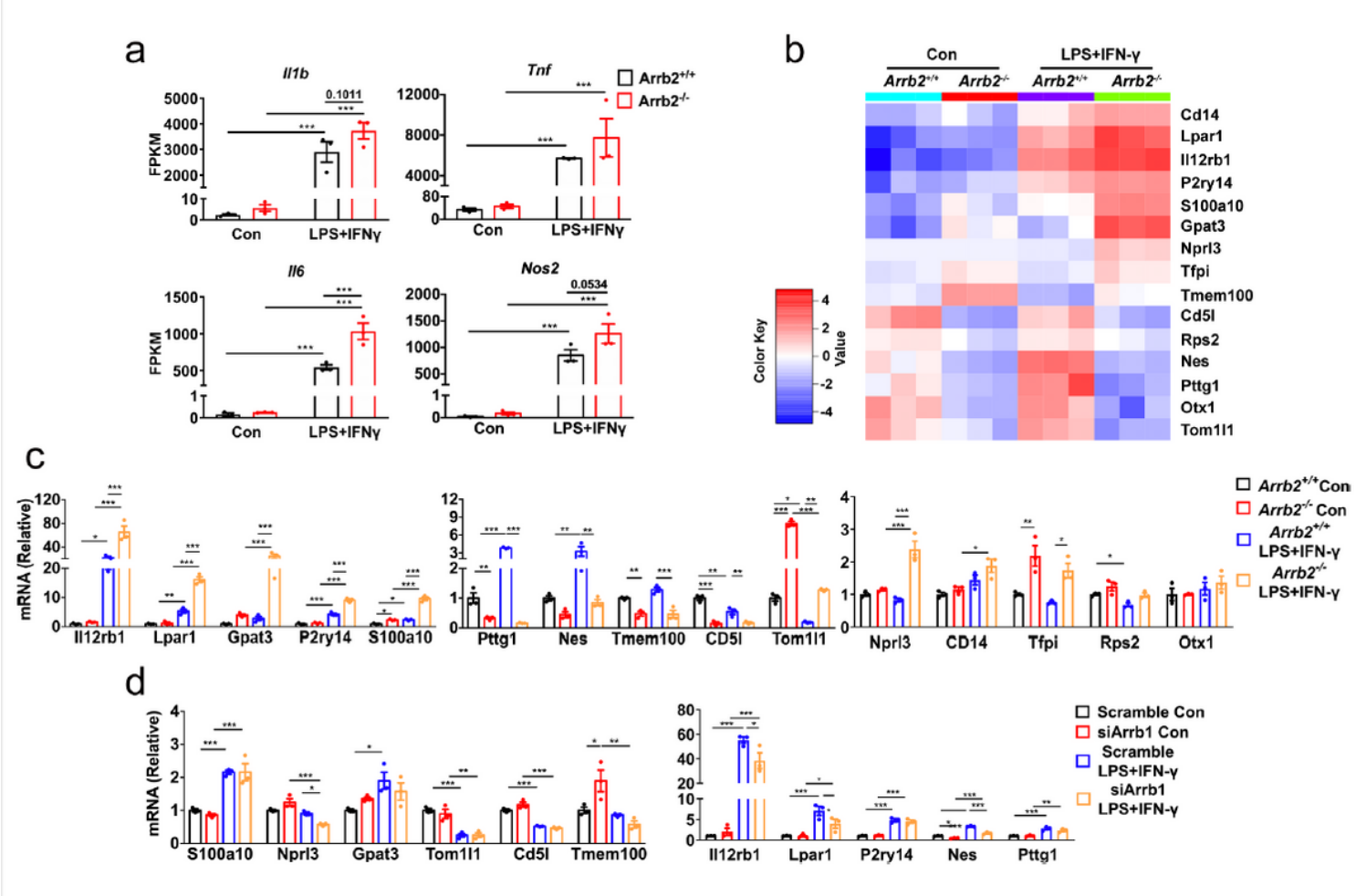

Figure 7

Effects of ARRB1 and ARRB2 on Nprl3 expression in microglia. a Normalized expression of pro-inflammatory markers measured by RNA-seq in microglia from WT and Arrb2-/- mice with or without LPS plus IFN-γ treatment for 6 h. b Heatmap of inflammatory genes in microglia from WT and Arrb2-/- mice. The genes shown are differentially expressed (padj≤0.05, log2-fold change ≥1 or ≤-1) in WT and Arrb2-/- mice. c Expression of 15 genes shown in b were measured by RT-PCR. d Gene expression in siRNA-mediated ARRB1 knockdown microglia. Quantitative data are mean ± s.e. (n = 3). *P < 0.05, **P < 0.01, and ***P < 0.001.

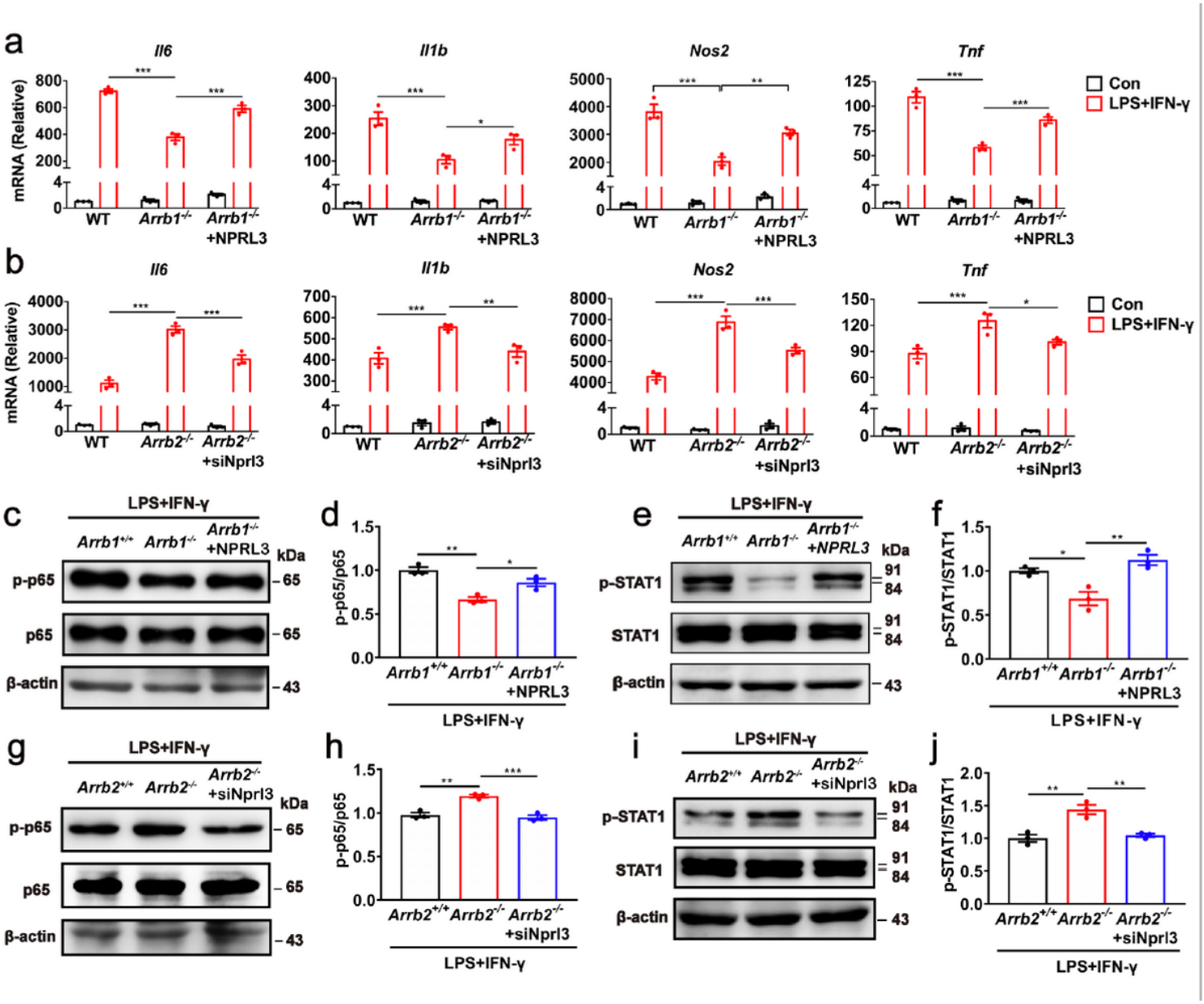

Figure 8

Effects of overexpression and knockdown of Nprl3 on ARRB-mediated microglia inflammation. a-b Inflammatory gene expression in microglia from WT and ARRB knockout mice after transfection with either NPRL3 for 24 (a) or Nprl3 siRNA for 48 h (b). c-j Activation of p65 (c, d, g and h) and STAT1 (e, f, i and j) in microglia after Nprl3 overexpression (c-f) or knockdown (g-j) as above. Quantitative data are mean ± s.e. (n = 3). *P < 0.05, **P < 0.01, and ***P < 0.001.

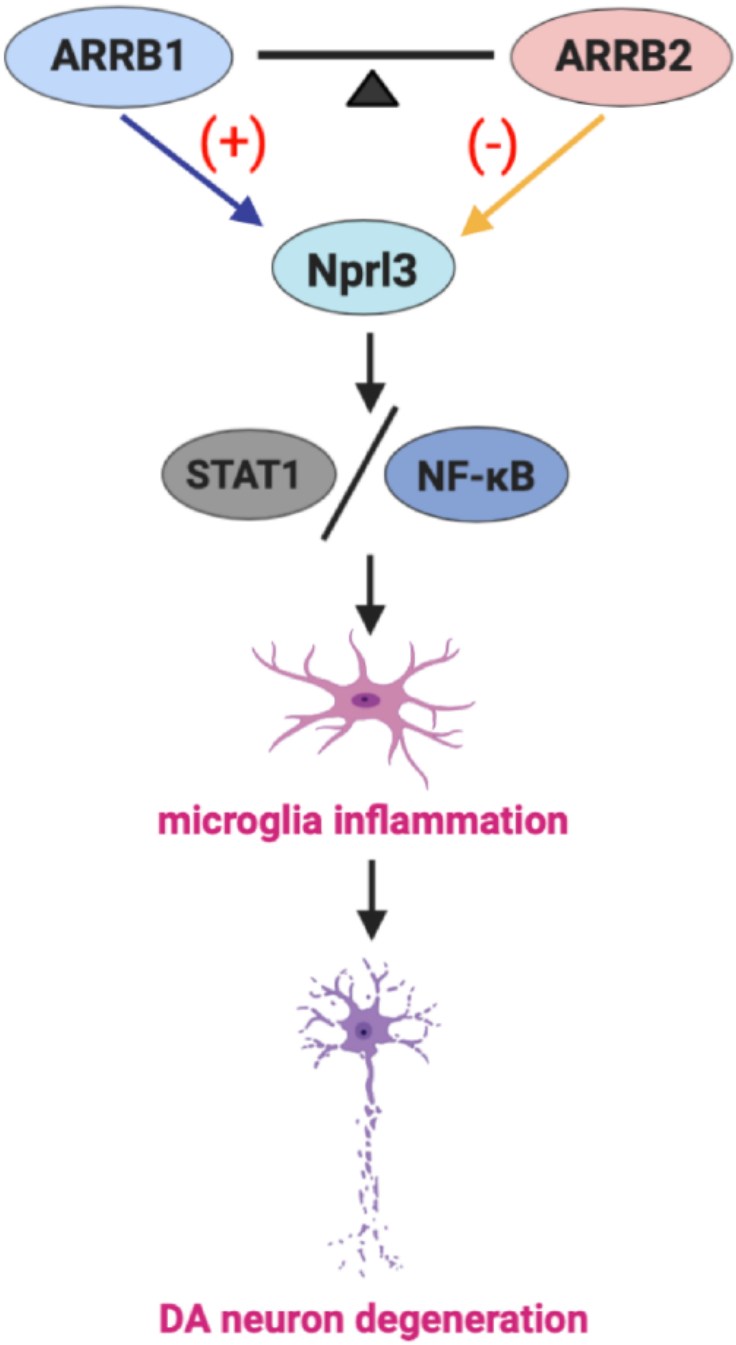

Figure 9

A schematic diagram showing the opposite roles of ARRB1 and ARRB2 in microglia-mediated inflammation and DA neuron degeneration via regulating Nprl3 and the inflammatory STAT1 and NF-κB pathways (see text for details). +, stimulatory; -, inhibitory.

Supplementary Files

This is a list of supplementary files associated with this preprint. Click to download.

- addtionalfile2tables2.xlsx
- figureS8.pdf
- figureS5.pdf
- figureS6.pdf
- figureS7.pdf
- figureS3.pdf
- figureS2.pdf
- figureS4.pdf
- additionalfile1tables1.xlsx
- figureS1.pdf